Composites Part B 107 (2016) 97–105

Contents lists available at ScienceDirect

Composites Part B

journal homepage: www.elsevier.com/locate/compositesb

Nanoparticle reinforcement in elastomeric polyethylene composites under tensile tests

Humberto Palza [a, *], Mauricio Rojas [a], Elizabeth Cortez [b], Rodrigo Palma [b], Paula Zapata [c]

[a] Departamento de Ingeniería Química y Biotecnología, Facultad de Ciencias Físicas y Matemáticas, Universidad de Chile, Chile
[b] Departamento de Ingeniería Mecánica, Facultad de Ciencias Físicas y Matemáticas, Universidad de Chile, Chile
[c] Grupo Polímeros, Facultad de Química y Biología, Universidad de Santiago de Chile, Chile

ARTICLE INFO

Article history:
Received 14 July 2016
Received in revised form
12 September 2016
Accepted 17 September 2016
Available online 20 September 2016

Keywords:
Nanocomposites
Nanoparticle reinforcements
Micromechanical models

ABSTRACT

Two ethylene-1-butene thermoplastic elastomer copolymers were melt mixed with different nanometric fillers such as: multi-walled carbon nanotubes (CNT), thermally reduced graphite oxide (TrGO), and spherical metal nanoparticles. The effect of both the kind and amount of nanoparticles on the tensile mechanical behavior of the matrices was evaluated focusing on the elastic modulus. The low elastic modulus of the pure elastomeric polymers, with values of 50 and 9 MPa depending on the amount of comonomer, can be largely increased by adding nanoparticles although the reinforcement was conditioned by the matrix and kind of filler. For instance, while CNT increased the elastic modulus of the stiffer matrix with a maximum of 80%, this property increased 4,3 times as compared with the pure matrix when added to the softer matrix. Noteworthy, TrGO particles rendered even larger improvements with composites based on the softer matrix reaching values as high as 7 times the modulus of the pure sample at concentrations less than 10 vol%. Spherical metal nanoparticles otherwise rendered outstanding improvements in the elastic modulus (around 60%) at concentrations as low as 2 vol%. These results were explained by micromechanical models stressing the relevance of both the aspect ratio and the mechanical properties of the particle agglomerates rather than of the isolated particles.

1. Introduction

Polymer nanocomposites provide an effective way to utilize the unique properties of nanoscale particles in bulk applications attracting a growing interest due to the very broad range of their current and projected applications. They often exhibit significant property changes at very low filler contents allowing to modify and to improve material performance without sacrificing excellent polymer processability and low density [1]. In particular, the mechanical properties are drastically enhanced in nanocomposites depending on the particle size, particle content and particle/matrix interfacial adhesion [2]. For instance, the modulus of polymer composites can be decreased by increasing particle size from 15 to 35 nm, especially at high particle loading [2].

A couple of decades ago, carbon nanotubes (CNT) emerged as the ideal filler candidate for advanced composites due to their unprecedented physical and chemical properties [3]. For instance, the elastic moduli of CNT are superior to all carbon fibres with values greater than 1 TPa while their strength can be as high as 63 GPa [4,5]. The latter is an order of magnitude stronger than high strength carbon fibres. Even the weakest type of CNT has strengths of several GPa [3]. Therefore, one of the most promising research areas of composites involves the mechanical enhancement of plastics using CNT as reinforcing fillers as they were visualized as the ultimate mechanical filler material [3]. However, in the last years both graphene and graphite derivatives appeared with even more outstanding behavior likely overcoming to CNT as ideal filler for polymer matrices. Graphene is considered a two-dimensional carbon nanofiller with a one-atom-thick planar sheet of sp2 bonded carbon atoms that are densely packed in a honeycomb crystal lattice [6]. It has been viewed as the building block of all other graphitic carbon allotropes of different dimensionality such as graphite (3-D carbon allotrope) that is made of graphene sheets stacked on top of each other [7]. With an elastic modulus of 1 TPa and ultimate strength of 130 GPa, single-layer graphene is the strongest material ever measured [8]. The superior mechanical properties of graphene compared to polymers also motivated the research in polymer/graphene nanocomposites [6]. Today, different

* Corresponding author.
E-mail address: hpalza@ing.uchile.cl (H. Palza).

http://dx.doi.org/10.1016/j.compositesb.2016.09.053
1359-8368/

graphene based materials can be used as filler in polymer matrices such as graphite nanoplatelet coming from graphite oxide or graphite intercalated compounds [9].

Some reports conclude the advantages of graphene over CNT in polymer mechanical reinforcement. For instance, by comparing three different carbon nanostructures, namely single wall CNT, expanded graphite (EG), and functionalized graphene sheets (FGS), the effect of the kind of carbon particles on the behavior of poly (methyl methacrylate) was discussed [10]. Surface functionality of FGS afforded better interaction with the polymer than unmodified CNTs or traditional EG, imparting higher mechanical improvements. In particular, while CNT increased the elastic modulus a 50%, FGS increased this property around 80% at 1 wt% of filler. The wrinkled single-sheet morphology of FGS, further explained this tendency. Similar conclusions were found in polypropylene, polycarbonate, and poly (styrene-co-acrylonitrile) matrices. By using thermally reduced graphite oxide (TrGO), the elastic modulus of these matrices was increased significantly (around 50%) as compared with CNT at 5 wt% of filler [11]. This tendency was also confirmed in epoxy nanocomposites mixed with CNT and graphene platelet at 0.1 wt% of filler [12]. At this low filler content, graphene rendered significant improvement in mechanical properties to the epoxy matrix (around 30%) as compared to CNT composites. Despite the relevance of these comparative results between CNT and graphene derivative fillers in polymer composites, similar studies using soft matrices such as elastomers are not yet available. This is even more relevant taking into account that these matrices display the largest improvements in mechanical behavior due to the stiffness contrast between reinforcement filler and matrix [7].

The addition of graphene based materials to elastomers can result in a material with positive elements of both hard thermoplastics and elastomers, such as high stiffness, strength, ductility, and toughness [13]. In elastomeric polyurethane/graphene composites, the elastic modulus increased by a factor of 100 by addition of high amount of graphene (around 50 wt%) [13]. Increases as high as 10-fold in the mechanical behavior of thermoplastic elastomeric polyurethane can be obtained by adding 3 wt% of chemical modified graphite oxide [14]. The formation of chemical bonding between polyurethane and graphite oxide nanoplatelets allowed an effective load transfer reaching increases in the elastic modulus around 900% at 4.4 wt% of filler [15]. Stiffer samples such as poly (vinyl alcohol) can also display outstanding improvements at 1.8 vol% of flat carbon nanosheets [16]. All the above mentioned elastomers present some polarity facilitating the filler/matrix interaction. Non-polar elastomers otherwise have not been extensively explored in this context despite their high relevance such as those derivate from polyethylene. Thermoplastic polyethylene elastomers (TPE) is a new class of material emerged from the development of constrained geometry catalyst based on homogeneous ethylene/olefin copolymers. The main advantage of these polymers over chemically vulcanized elastomers lies in their processing and post-processing behavior that is as similar as conventional polyethylenes [17]. These polymers present controlled topology and therefore tailor-made properties allowing the design of material with significant flexibility, strength and durability [18]. In addition, TPE has the ability to elongate under stress, allowing them to maintain their integrity under localized differential settlement conditions without puncturing, tearing or cracking [19]. The presence of short-chain branching further improves the interaction with nanoparticle such as natural clay [20]. With the addition of carbon particles, a mechanical reinforcement can be obtained associated with a good particle–TPE adhesion. The stress–strain curves scaled with that of the unfilled polymer even at large strains suggesting good filler–matrix adhesion [17]. The final mechanical behavior depended on the characteristics of the carbon filler as composites with high-structured carbon black fillers retained the inherent high elongation of the unfilled elastomer even at 30 vol% [18]. TPE/CNT composites are barely reported, despite these carbon nanostructures are able to enhance the mechanical behavior of the matrix [21]. However, the moduli of these composites were slightly lower than those using carbon fibers [21]. Modified graphene was also used as filler in a TPE composites prepared by solution mixing although the improvements were much lower than those obtained for traditional elastomers despite the low elastic modulus of the matrix (around 3 MPa) [22]. A much larger increase was obtained by using thermally reduced graphene oxide mixed with TPE by either melt or solvent mixing [23]. TPE increased its elastic modulus around 80% at 5 wt% although by either functionalizing the TPE or by using the solvent method, these values were increased.

Metal filled polymer composites otherwise are widely used for electromagnetic interference shielding and bio-application as they have a lighter weight than metals and are less costly [24–26]. In general, copper metal nanoparticles can be used for both family of applications due to their electrical conductivity and antimicrobial characteristics. Composites prepared using low density polyethylene with copper nanoparticles presented a strong effect of the metal size on the mechanical behavior and while copper nanoparticles increased the elastic modulus of the resulting composites, microparticles presented the opposite tendency [25]. However, other article reported that the addition of microparticles increase the stiffness of both low and high density polyethylene [24]. To our knowledge, comparative studies regarding the effect of these metal nanoparticles with other fillers have not been performed.

Based on the above mentioned, there is a lack of comparative studies about the effect of different kind of nanoparticles, such as those based on either carbon or metal, on the mechanical behavior of elastomeric polymers, for instance in thermoplastics. The goal of the present article is therefore to analyze the effect of different nanostructures on the tensile mechanical behavior of two TPE having different stiffness. In particular, two ethylene-1-butene thermoplastic elastomer copolymers were melt mixed with: multi-walled carbon nanotubes (CNT), thermally reduced graphite oxide (TrGO), and spherical metal nanoparticles. Our results showed that a dramatic increase in the elastic modulus can be obtained despite the low polarity of the matrix, and this increase depended on both the matrix and the nanoparticle with TrGO particles displaying the largest improvements. These results were discussed by using micromechanical models stressing the relevance of filler final agglomeration state.

2. Experimental

2.1. Materials

Two commercial grade ethylene-1-butene copolymers from Dow Chemical were used as the polymer matrix, named E1 (commercial code HM7289) and E2 (commercial code HM7387). Based on the datasheet information provided by Dow, the densities, the total crystallinity and the melting temperatures are 0.891 and 0.870 g/cm3, 28 and 16%, and 99 and 50 °C, for E1 and E2, respectively. Based on this information, the higher incorporation of 1-butene in E2 than E1 is concluded based on the relationship between comonomer content and both crystallinity and melting temperature [27,28]. Moreover, based on experimental results from similar copolymers, the comonomer content can be roughly estimated around 6 and 14 mol% for E1 and E2, respectively.

Extra pure graphite powders (G), sulfuric acid (98.08%, H2SO4), potassium permanganate (99%, KMnO4), Hydrochloric acid (32%, HCl), and sodium nitrate (99.5%, NaNO3), were obtained from

Merck (Germany) and used as received. Hydrogen peroxide (5%, H2O2) was purchased from Kadus S.A. Thermally reduced graphite oxide (TrGO) was prepared in a two-step oxidation/thermal reduction process using G as raw material. The graphite oxidation process of Hummers and Offeman was employed as detailed elsewhere [29,30]. The first step is an oxidation of G with KMnO4 and NaNO3 in concentrated sulfuric acid obtaining a graphite oxide (GO). In a second step, the dry GO was thermally reduced to afford thermally reduced graphite oxide (TrGO) in a nitrogen atmosphere by rapidly heating GO up to 600 °C during 40 s using a quartz reactor heated in a vertical tube furnace. Multi wall carbon nanotubes (MWCNT) (Baytubes C150P) were obtained from Bayer Material Science AG (Germany). Based on the datasheet information provided by Bayer, they are characterized by a purity higher than 95 wt%, number of walls between 2 and 15, an outer mean diameter of 13–16 nm, an inner mean diameter of 4 nm, length between 1 and > 10 μm, and a bulk density around 150 kg/m^3. Metal copper nanoparticles were obtained from Suzhou Canfuo Nanotechnology Co. Based on the data sheet they present spherical morphology with sizes between 50 and 600 nm.

2.2. Composite preparation and characterization

The composites were prepared by using a Brabender Plasticorder (Brabender, Germany) internal mixer at 170 °C and a speed of 110 rpm. Filler content ranges from 0 to 9 vol% for TrGO or CNT. First, a half of polymer and an antioxidant were added to the mixer operated at 110 rpm. After 2 min approximately for melt the polymer, the filler was added during 3 min. Finally, the rest of polymer pellets was added and the speed of the mixer was held at 110 rpm for 10 min. Therefore, the total mixing time was around 15 min. Afterward, the samples were press molded at 170 °C at 50 bar for 5 min and cooled under pressure by flushing the press with cold water, in order to obtain the final samples for tests. The samples were cut with a stainless steel mold with dimensions according to type IV (ASTM D638) with 1 mm of thickness. After sample preparation, the materials were left at room temperature by at least three days allowing crystallization of the highly amorphous polymer by annealing.

The melting endotherms were obtained using a Mettler Toledo DSC1/500 differential scanning calorimeter (DSC) under N2 atmosphere to minimize thermal degradation. The samples were heated from 25 to 200 °C at a heating rate of 10 °C/min. For crystallinity measurements, the heat of fusion of completely crystalline polyethylene was assumed to be 293 J/g [31]. The mechanical properties were measured using a HP D500 dynamometer at a rate of 50 mm/min at 23 °C and 30% relative humidity. A minimum of three samples were tested for each material and the average values are reported. The experimental error was about 6% relative to the mean value. The morphology of the composites was analyzed using a field emission scanning electron microscope (FEI-SEM Inspect 50) by covering the sample with a gold layer.

3. Results

3.1. Carbon nanostructures

Fig. 1 displays the tensile stress-strain curves for the different matrices and their composites with either carbon nanotube (CNT) or thermally reduced graphite oxide (TrGO). Regarding the pure matrices, the presence of 1-butene in the main chain was able to disrupt the crystal structure of the polyethylene drastically decreasing its crystallinity as observed in Table 1. The crystallinities measured were less than 5% even after room temperature annealing where some amorphous entities not able to crystallize during cooling can do it [32]. The non-inclusion of comonomer within crystallites hinders the chain regularity needed for the crystallization and therefore reduces the length of the main chain able to crystallize. Consequently, the crystallinity degree of these copolymers was lowered [32]. The crystallinity drops was the main reason for the low elastic modulus of pure matrices under tensile conditions. The tests were carried out at room temperature behaving the amorphous region of the polymer like a viscoelastic liquid with poor stiffness [20]. For instance, the matrix with the highest amount of comonomer (E2) displayed both the lowest elastic modulus (9 MPa) and the highest elongation at break (>400%) as compared with the E1 matrix with a modulus of 50 MPa and elongation at break around 350%. Fig. 1 further shows that the pure matrices presented a broad yield point and a large strain-hardening elongation without cold-drawing that has been previously associated with a semi-elastomeric behavior. This behavior is explained by the presence of tie chains in the copolymers transferring efficiently the tensile energy through the sample avoiding stress concentrations in specific points [20,33].

From Fig. 1 is concluded that the presence of carbon nanostructures has a significant effect on the tensile mechanical behavior of the matrices. In general, by increasing the amount of carbon nanoparticles the sample became stiffer meaning larger stresses for reach a certain strain. In this way, they were able to partially compensate the drop in the elastic modulus as summarized in Fig. 2 displaying the relative modulus defined as the ratio between the elastic modulus of the composite and the elastic modulus of the pure matrix. These results further show that the mechanical improvement highly depended on the matrix characteristic and the type of carbon nanostructures with both the softer matrix and TrGO displaying the largest changes. Composites based on E1 with CNT have elastic modulus increased a 50% meanwhile with TrGO these improvements increased a factor of 2, at around 5 vol% of filler. The stiffness of E1/TrGO composites was further increased by raising the amount of filler reaching values as high as a factor of 4 at 10 vol%. By using E2 matrix, these changes were even more drastic with CNT improving the elastic modulus by a factor of 3,0 while with TrGO a factor of 5 is obtained at the same amount of filler (around 8 vol%). By increasing the amount of TrGO the composite was stiffer by a factor of 7,0 at 9 vol% of filler. However, the increase in the stiffness also was associated with a reduction in the elongation at break of the samples as previously reported for either CNT or TrGO polymeric composites [11,13,14,16,18,22,34,35]. Both the restrictions of polymer movements due to the particles and the premature failure starting at the particle aggregates seem to explain this tendency [16,34].

To understand the large improvements in the stiffness of the composites, the effect of the carbon nanostructures on the polymer crystallinity should be analyzed as nanoparticles can nucleate the crystallization of polymers [7,36]. As above mentioned, changes in crystallinity can explain modifications in the elastic modulus of the composites. Table 1 shows the melting enthalpy and the crystallinity of the samples allowed us to rule out an increase in the crystallinity associated with the presence of the carbon nanostructures. Moreover, some composites displayed lower crystallinity than pure matrix as reported previously in similar systems [22]. This contradictory trend has been found in previous reports due to a suppressed crystallization by the nanoparticle [7]. The reason was associated with the formation of a random polymer/particle interface inhibiting the formation of ordered crystalline structure of polymer chains [22]. Based on these results, hereafter we only focused on the mechanical contribution of filler into the polymer matrix assuming that the mechanical behavior of the matrix is unchanged.

Based on the above mentioned, the addition of carbon

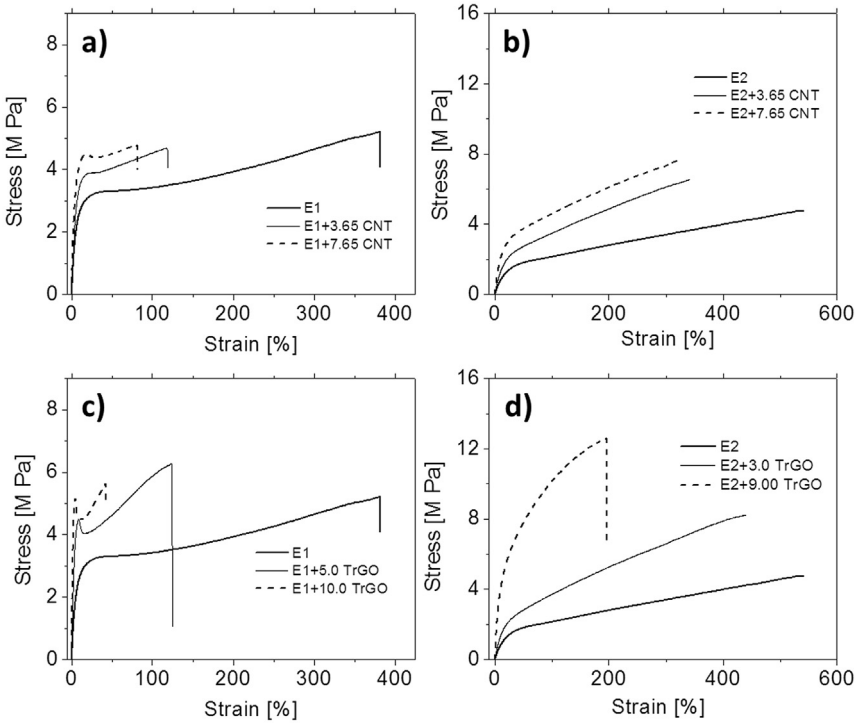

Fig. 1. Tensile stress-strain tests for the different samples: a) pure E1 and its composites with CNT; b) pure E2 and its composites with CNT; c) pure E1 and its composites with TrGO; and d) pure E2 and its composites with TrGO.

Table 1
Melting enthalpy and crystallinity of the different samples measured by dynamic scanning calorimetry test. The crystallinity was measured as the ratio between the experimental enthalpy and the 100% crystalline polyethylene (293 J/g).

Matrix	Filler	Concentration [wt%]	Melting enthalpy [J/g]	Crystallinity [%]
E1	N/A	N/A	7,6	2,6
	CNT	3.7	7,0	2,4
		4.6	6, 8	2,3
		5.6	8,2	2,8
		7.8	9,0	3,1
	TrGO	2.0	5,4	1,9
		3.0	5,2	1,8
		5.0	11,3	3,9
		9.0	11,6	4,0
		10.0	8,6	3,0
E2	N/A	N/A	8,8	3,0
	CNT	3.7	8,2	2,8
		5.6	7, 6	2,6
		6.6	7,7	2,7
		7.6	5,0	1,7
	TrGO	2.0	8,0	2,8
		3.0	7,9	2,7
		5.0	7,4	2,6
		6.6	6,0	2,1
		7.6	5,2	1,8

nanoparticles into TPE matrices drastically enhanced the elastic modulus of the original matrices because of the reinforcement effect of the filler. However, these results should be analyzed in the context of the maximum improvement reached with nanoparticles embedded in soft matrices as expected by theoretical models. Therefore, to further understand these experimental results, micromechanical models were applied. In particular, the Halpin-Tsai model was used to approximately predict the modulus of composites, as previously reported in polymer composites, in particular based on fibers or carbon nanostructures [11,35,37–40].

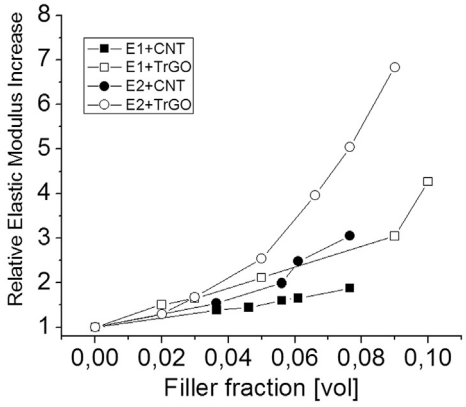

Fig. 2. Effect of the polymer matrix, filler, and its concentration on the relative elastic modulus increase of the samples defined as the ratio between the elastic modulus of the composite and the elastic modulus of the pure matrix.

For random oriented fillers, the final equation for the elastic modulus of the composite (E_C) is based on the values for oriented filler in the longitudinal (E_L) and transverse (E_T) directions, measured as:

$$\frac{E_L}{E_M} = \frac{1 + 2 \cdot A \cdot \phi \cdot \eta_L}{1 - \phi \cdot \eta_L} \quad (1)$$

$$\frac{E_T}{E_M} = \frac{1 + 2 \cdot \phi \cdot \eta_T}{1 - \phi \cdot \eta_T} \quad (2)$$

$$\frac{E_C}{E_M} = \frac{3}{8}\frac{E_L}{E_M} + \frac{5}{8}\frac{E_T}{E_M} \quad (3)$$

where E_M is the elastic modulus of the pure matrix; ϕ is the volumetric fraction of filler; and A is the particle aspect ratio. η is defined by:

$$\eta_L = \frac{E_f - E_M}{E_f + 2 \cdot A \cdot E_M} \tag{4}$$

$$\eta_T = \frac{E_f - E_M}{E_f + 2 \cdot E_M} \tag{5}$$

where E_f is the elastic modulus of the filler.

These simple equations allowed us to understand the general tendency in elastomeric composites as these matrices can be considered soft meaning low elastic modulus and therefore large differences in stiffness as compared with the filler. Fig. 3 shows the theoretical effect of the matrix stiffness on the relative elastic modulus of composites based on equation (3), for the particular cases of 0.05 vol fraction of CNT and TrGO fillers. The elastic modulus used for CNT and TrGO were 0.45 and 1.00 TPa, respectively [12]. For composites with CNT, individual filler particles were assumed meaning an aspect ratio of 1000, whereas for composites with TrGO two aspect ratios were assumed: 60 and 600, representing the complex morphology of these particles in the composites. Fig. 3 show that by decreasing the elastic modulus of the matrix (values lower than 100 MPa approximately) the filler can reach the maximum contribution to the composite. Our matrices displayed elastic modulus in this region explaining the large improvements as compared for instance with standard thermoplastic such as linear polyethylene or polypropylene having elastic modulus around 1 GPa. It is relevant to analyze the case of matrices filled with low aspect ratio particles and high stiff filler, as in this case equations (4) and (5) became approximately equal to the unity, and therefore equation (3) can be considered independent of the matrix modulus. This is the case of composites based on TrGO with low aspect ratio as displayed in Fig. 3, stressing the relevance of the dispersion state of the filler. Noteworthy, even isolated CNT present a region where the mechanical improvement is independent of the elastic moduli of the matrix. Fig. 3 shows that this region belong to matrices with elastic moduli less than 100 MPa as in the case of our matrices, therefore the larger improvement in composites based on E2 as compared with E1 can not be explained by their different elastic modulus. As below discussed, the difference can be rather explained by changes in the filler agglomeration.

By assuming well dispersed random CNT into the polymer matrix, equation (3) predicts increases in the elastic modulus much higher than the experimental findings, as displayed in Fig. 4 ("H-T" values). For instance, at a filler volume fraction of 0.004 the elastic modulus of the composites is predicted to increase by a factor of 3,5 and 4,0, for E1 and E2 matrices, while the experimental results showed that even at filler fraction of 0.08 these values were considerable lower (1,8 and 3,0, respectively). Therefore, the experimental improvements in elastic modulus are high but lower than theoretical predictions. The reason is associated with the distribution of CNT that is non-uniform through the matrix with local regions having higher concentration of filler than the average (Fig. 5). These regions with concentrated CNT are associated with agglomerates having a lower aspect ratio than the isolated filler. Moreover, polymer molecules are incorporated as observed in Fig. 5a. These "inclusions" have therefore different elastic properties as compared with both the surrounding material and the isolated CNT.

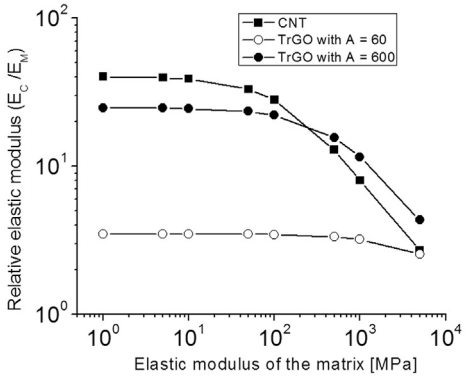

Fig. 3. Effect of both the polymer matrix stiffness and the carbon filler aspect ratio (A) on the relative elastic modulus increase based on the Halpin-Tsai model.

Under this condition, the development of a two-parameter model of agglomeration is possible in order to quantify this phenomenon [41,42]. By using the Voigt model and assuming both spherical inclusions and isotropic filler and matrix, the elastic properties of the inclusion and matrix can be estimated. In particular, the effective modulus of inclusions E_{in} and their surrounding E_{out} are [41]:

$$E_{in} = \frac{3}{8 \cdot \varepsilon_1}\{\phi \cdot \varepsilon_2 \cdot E_{CNT} + (\varepsilon_1 - \phi \cdot \varepsilon_2) \cdot E_{CNT}\} + \frac{5}{8} \cdot \frac{\varepsilon_1 \cdot E_{CNT} \cdot E_M}{(\varepsilon_1 - \phi \cdot \varepsilon_2) \cdot E_{CNT} + \phi \cdot \varepsilon_2 \cdot E_M} \tag{6}$$

$$E_{out} = \frac{3}{8}\left\{\left(\frac{\phi \cdot (1-\varepsilon_2)}{1-\varepsilon_1}\right) \cdot E_{CNT} + \left(1 - \frac{\phi \cdot (1-\varepsilon_2)}{1-\varepsilon_1}\right) \cdot E_M\right\} + \frac{5}{8}\left\{\frac{(1-\varepsilon_1) \cdot E_{CNT} \cdot E_M}{[(1-\varepsilon_1) - \phi \cdot (1-\varepsilon_2)] \cdot E_{CNT} + \phi \cdot (1-\varepsilon_2) \cdot E_M}\right\} \tag{7}$$

where ε_1 is the ratio between the volume of the spherical inclusions and the total volume; ε_2 is the ratio between the volumes of CNT dispersed in the inclusions and the total volume of CNT in the system; and E_{CNT} is the elastic modulus of CNT. These equations can be added to the Halpin-Tsai model for spherical particles meaning A = 1. When $\varepsilon_1 = \varepsilon_2$, CNT are dispersed uniformly into the matrix and the ratio between this value and the value when $\varepsilon_1 < \varepsilon_2$ is considered as the corrective factor to be applied into equation (3). Fig. 4 displays The modified values for medium ($\varepsilon_1 = 0.05$ and $\varepsilon_2 = 0.98$) and high ($\varepsilon_1 = 0.02$ and $\varepsilon_2 = 0.99$) agglomerate levels are displayed in Fig. 4 as "H-T mod1" and "H-T mod2", respectively. For high heterogeneous systems, the modified model was able to fit the experimental values meaning that the agglomeration of CNT is the responsible for the final reinforcement of the filler. Moreover, the prediction of the model with $\varepsilon_1 = 0.02$ and $\varepsilon_2 = 0.99$ fits properly the experimental results from E1 composites but for E2 composites did not fit at high filler concentrations and rather less agglomerated state should be assumed. Therefore, changes in the dispersion state between E1 and E2 could explain the effect of the matrix in the reinforcement effect, as below discussed in more details. These results confirm that the low reinforcement effect of CNT, as compared with theory, is associated with the spherical inclusions coming from the filler agglomeration decreasing the its aspect ratio as summarized in Fig. 3. The spherical-like morphology of the polymer/CNT inclusions can be observed in Fig. 5a displaying a SEM image of the E1 composites having 7,6 vol% of CNT.

For composites based on TrGO, we should consider that individual graphene sheets are barely observed in these samples based on exfoliation melt processes and rather stacks of several sheets are currently displayed [19,33]. By assuming isolate graphene sheets as

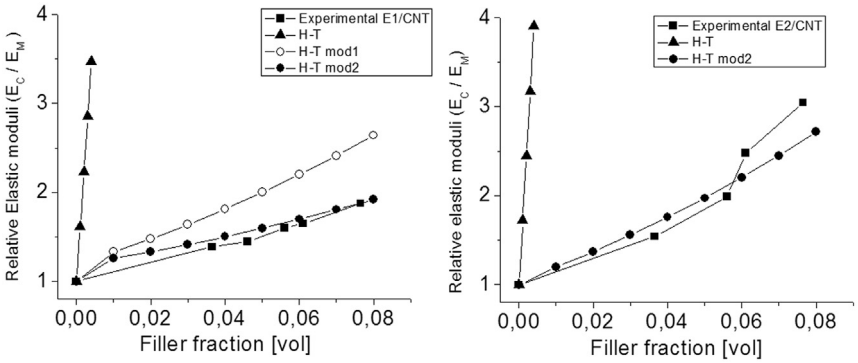

Fig. 4. Effect of the concentration of CNT on the relative elastic moduli of E1 (left-side) and E2 (right-side) matrices. The experimental results are displayed together with: a) results from the Halpin-Tsai model assuming isolated CNT in the composites (H–T); and b) modified Halpin-Tsai model assuming that CNT form inclusions with $\varepsilon_1 = 0.05$ and $\varepsilon_2 = 0.98$ (H-T mod 1) and $\varepsilon_1 = 0.02$ and $\varepsilon_2 = 0.99$ (H-T mod 2). See text for details regarding the models.

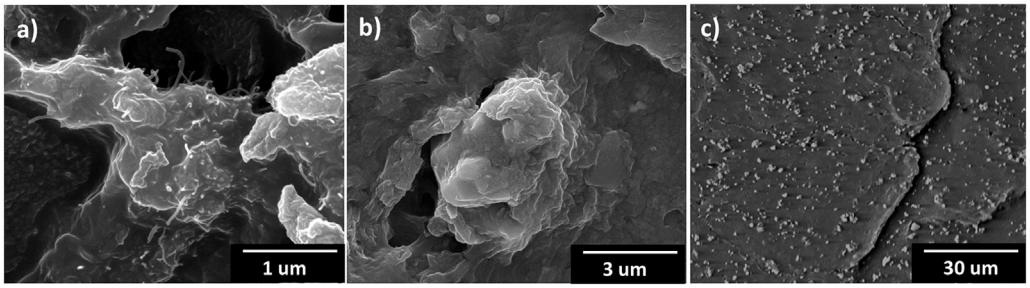

Fig. 5. Scanning electronic images (SEM) from some composites showing the agglomeration state of the different particles: a) E1 filled with 7.6 vol% of CNT; b) E1 filled with 9.0 vol% of TrGO; and c) E2 filled with 4.0 vol% of copper nanoparticles.

reported previously at low concentration of graphene, unrealistic high values are predicted by the models as displayed in Fig. 6 for A = 3000. It is well known that by increasing the concentration of this filler, the agglomeration degree is raised [16] and therefore the real value of A should be much lower than 3000 and the best fit was for values of A lower than 100 as displayed in Fig. 6. Therefore, the low aspect ratio of TrGO in the composites (Fig. 5b) as compared with the ideal case (isolate grapheme sheets) explained the results from these samples, similar to polymer/CNT composites. The latter meaning a poor delamination process during the melt mixing. However, even if TrGO is not completely delaminated, it presents a platelet-like morphology rather than spherical-like, meaning a larger aspect ratio than CNT inclusions. This difference in the aspect ratio explained the larger reinforcement of graphite derivatives.

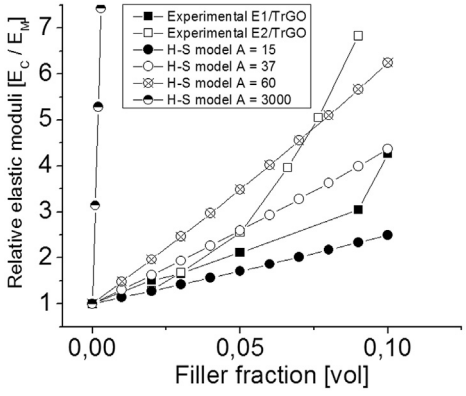

Fig. 6. Effect of the concentration of TrGO on the relative elastic moduli of E1 and E2 matrices. The experimental results are displayed together with results from the Halpin-Tsai model (H–S model) assuming different aspect ratio of the particle (A).

Regarding the effect of the polymer matrix, as above concluded, when particles with low aspect ratio and high stiffness are used (Fig. 3), the models are independent of the elastic modulus of the matrix, and therefore Fig. 6 just displays the model results from one matrix. Despite the latter, compared with composites based on CNT, there is a larger effect of the polymer matrix in the mechanical behavior of TrGO composites with those based on E2 displaying the highest elastic modulus. The best fits were obtained assuming aspect ratios between 15 and 37, and 37 and 60, for composites based on E1 and E2, respectively, Therefore, the larger improvements associated with E2 are associated with a better particle dispersion meaning higher aspect ratio. The agglomerates can be infiltrated by low viscous polymers affecting either the packing structure or the cohesive forces binding small agglomerates [43–45]. It seems that the presence of short chain branching, reducing the viscosity of the matrix, increased the interaction with the agglomerates reducing its sizes [46]. Similar results were reported for polypropylene with short chain branching melt mixed with natural clays [20]. This infiltration phenomenon has also been reported in polypropylene composites based on carbon nanotubes meaning that the higher improvements observed in E2/CNT composites as compared with E1/CNT composites can also be explained by this process [47].

3.2. Spherical metal nanoparticles

To further extent our discussion regarding the tensile mechanical behavior of soft elastomeric nanocomposites, the matrices were melt mixed with spherical copper metal nanoparticles. Unlike platelet- and CNT-reinforced nanocomposites that usually underperform as compared to theoretical predictions regarding

mechanical properties, this kind of nanoparticles often exhibit stiffness higher than those predicted by the models [1]. The addition of relatively small amounts of inorganic spherical-like particles such as silica, titania, or calcium carbonate having dimension in the nanometer scale was proven to increase both rigidity and toughness of different thermoplastics [1,48,49]. Fig. 7 displays the results for the relative modulus obtained by adding low amount of copper nanoparticles into both matrices. In these samples, the elastic modulus was able to increase considerable and for 2 vol% of filler the stiffness increased around 40 and 60% for E1 and E2, respectively, confirming the relevance of the polymer matrix. Noteworthy, unlike carbon nanostructured fillers the increase in the stiffness of the composites with spherical nanoparticles was higher than the predicted by the Halpin-Tsai model (around 6%). The composites with metal nanoparticles displayed increases as similar as composites with TrGO, despite the different particle morphology. Another difference is the effect of the filler concentration as by increasing the amount of particles, the stiffness level-off.

Several theories tried to understand the outstanding improvements in stiffness at low concentration of spherical nanofillers [1]. The interaction between the particle and the polymer molecules is stated as the mechanism behind the experimental findings. Nanoparticles restrict the mobility and deformation of the matrix by introducing a mechanical restraint [2]. The restriction in polymeric molecular diffusion in the presence of solid particles occurs because of an effective attraction potential between segments of the chain and the repulsive potential that the polymer is subjected to when it is close to solid particles [2]. However in our case this can be ruled out due to the non-polar nature of the polyethylene. An alternative explanation able to fit the experimental stiffness was recently reported based on the agglomeration of the nanoparticles [1]. Nanoparticles have high specific surface area and are prone to agglomerate due to strong interparticle interaction. Deformation of the matrix confined within these rigid aggregates is constrained due to the aggregate reinforcing effect, as opposed to the unconstrained (bulk) matrix outside the aggregates. The matrix in the composite can therefore be divided into two parts: constrained matrix and unconstrained bulk matrix. If the primary nanoparticle aggregation is considered as the main mechanism for this process, a new parameter can be defined: constrained matrix ratio (α), equal to the ratio between the constrained matrix fraction (m) and the filler volume fraction (V):

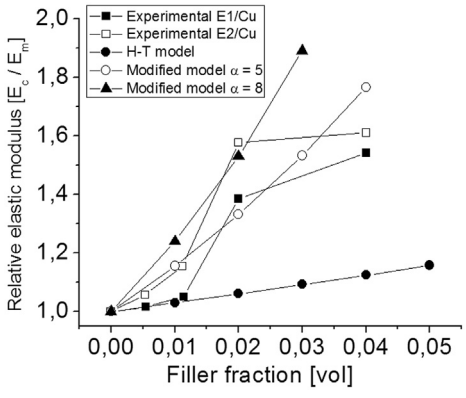

Fig. 7. Effect of the concentration of spherical copper nanoparticles (Cu) on the relative elastic moduli for E1 and E2 matrices. The experimental results are displayed together with: a) results from the Halpin-Tsai model assuming isolated Cu particles in the composites (H-T model); and b) modified model assuming agglomeration of particles where polymer molecules are constrained. In the latter model, the constrained matrix ratio (α) is added into the model.

$$\alpha = \frac{m}{V} \quad [8]$$

Based on this parameter, the volume content of the inclusions is defined as V' = V + M = V*(1+α). With these concepts, the bulk (K) and shear (G) modulus of the agglomerated nanocomposites can be estimated by Ref. [1]:

$$K = K_m + \frac{V' \cdot \left(K_f - K_m\right)}{1 + (1 - V') \cdot R_m \cdot \left(K_f - K_m\right) + R} \quad [9]$$

$$G = G_m + \frac{V' \cdot \left(G_f - G_m\right)}{1 + (1 - V') \cdot Q_m \cdot \left(G_f - G_m\right) + Q} \quad [10]$$

$$E = \frac{9 \cdot K \cdot G}{3 \cdot K + G} \quad [11]$$

Where:

$$R = \frac{\alpha}{1 + R_f \cdot \left(K_m - K_f\right)} \quad [12]$$

$$Q = \frac{\alpha}{1 + Q \cdot \left(G_m - G_f\right)} \quad [13]$$

K_f and G_f, and K_m and K_f represent the bulk and shear modulus of the filler and matrix respectively. These parameters were evaluated from:

$$K = \frac{E}{3 - 6 \cdot \nu} \quad [14]$$

$$G = \frac{E}{2 + 2 \cdot \nu} \quad [15]$$

where ν and E are the Poisson ratio and elastic modulus of the material with values of 131 GPa and 0,351 for copper [50]. Although 0,5 is the current value assumed for our matrices [18,51], a Poisson ratio of 0,49 was assumed avoiding the mathematical singularity in K. R_i is a constant related with the modulus of either the matrix (R_m in equation (9)) or the filler (R_f in equation (12)), measured by:

$$R_{i=\frac{3}{3K_i+4G_i}} \quad [16]$$

Fig. 7 displays the results obtained from this model assuming different values of α: 5 and 8. Unlike the previous models, in this case by taking into account constrained polymer molecules presenting inside the agglomerates of the particles, the stiffness of the composite is increased much more than by standard Halpin-Tsai model.

The models presented here shows that the agglomeration can have two independent consequences: 1) decrease the aspect ratio of the filler as occurring for CNT and TrGO and represented by equations (3) and (6) and (7), respectively, and 2) constrains the polymer molecules inside the agglomerates as occurring in spherical particles and represented by equations (9) and (10). A possible explanation of why in spherical particles equations (9) and (10) properly represent the increasing stiffness of the composites as compared with Halpin-Tsai can be related with the fact that the agglomerates in this case have the same aspect ratio of the individual filler and therefore there is no a reduction of the relative stiffness associated with lower aspect ratios of the agglomerates.

The latter occurring in high aspect ratio individual particles such as CNT and graphene.

Although not applied in this contribution, the micromechanical analysis of our experimental results can be extended by taking into account either models already used for similar thermoplastic elastomer materials, such as the Guth analysis [17], or more advanced theories. For instance, a three-parameter viscoplasticity model developed for polymer composites was able to predict not only their stress-strain response but also their non-linear rate-dependent behavior [52]. In polymer/CNT composites, both the equivalent-continuum modeling and the self-similar approach were able to incorporate information about molecular interactions at the nanometer length scale [53]. A recent model developed for inorganic nanocomposites (silicon with Al_2O_3-nanoparticles), based on the modified strain gradient theory, resulted in a size-dependent micromechanical model for multi-phase materials [54]. In particular, the effect of the surface energy of the inhomogeneities inside the composite structure was incorporated into the micromechanical model. Therefore, further studies are needed to apply models able to incorporate the effect not only of the filler agglomeration but also of the filler size and polymer/particle interaction.

4. Conclusions

By mixing different nanoparticles with two elastomeric polyethylene matrices relevant information regarding the effect of the kind of nanoparticle on the mechanical reinforcement of composite was obtained. The addition of nanoparticles into soft matrices drastically improved their elastic modulus with improvements as high as 7-folds relative to the pure matrix. The softer polymer matrix displayed larger improvements in the elastic modulus likely associated with a better particle dispersion into the matrix because of its low viscosity. Composites based on CNT presented much lower mechanical reinforcement than predictions from micromechanical models because of the spherical-like agglomeration state of the filler observed in the composites, reducing dramatically its effective aspect ratio. Agglomerates in TrGO composites otherwise presented a platelet-like morphology explaining the observed higher reinforcement effect than CNT composites. When spherical nanoparticles were used as filler a different tendency was found as in this case the model predict lower values than experimental results. Micromechanical models showed that the agglomerations are relevant in the mechanical reinforcement effect because they have both constrained polymer molecules inside and lower effective aspect ratio than isolated particles.

Acknowledgments

The authors gratefully acknowledge the financial support of CONICYT, project FONDECYT 1150130. It is also expressed the thanks to Dr. C. Garzón for the support during this research.

References

[1] Dorigato A, Dzenis Y, Pegoretti A. Filler aggregation as a reinforcement mechanism in polymer nanocomposites. Mech Mater 2013;61:79–90.
[2] Fu SY, Feng XQ, Lauke B, Mai YW. Effects of particle size, particle/matrix interface adhesion and particle loading on mechanical properties of particulate–polymer composites. Compos Part B 2008;39:933–61.
[3] Coleman JN, Khan U, Blau WJ, Gun'ko YK. Small but strong: a review of the mechanical properties of carbon nanotube–polymer composites. Carbon 2006;44:1624–52.
[4] Wong EW, Sheehan PE, Lieber CM. Nanobeam mechanics: elasticity, strength, and toughness of nanorods and nanotubes. Science 1997;277:1971–5.
[5] Yu M, Lourie O, Dyer MJ, Kelly TF, Ruoff RS. Strength and breaking mechanism of multiwalled carbon nanotubes under tensile load. Science 2000;287:637–40.
[6] Kuilla T, Bhadra S, Yao D, Kim NH, Bose S, Lee JH. Recent advances in graphene based polymer composites. Prog Polym Sci 2010;35:1350–75.
[7] Kim H, Abdala AA, Macosko CW. Graphene/polymer nanocomposites. Macromolecules 2010;43:6515–30.
[8] Lee C, Wei X, Kysar JW, Hone J. Measurement of the elastic properties and intrinsic strength of monolayer graphene. Science 2008;312:385–8.
[9] Potts JR, Dreyer DR, Bielawski CW, Ruoff RS. Graphene-based polymer nanocomposites. Polymer 2011;52:5–25.
[10] Ramanathan T, Abdala AA, Stankovich S, Dikin A, Herrera-Alonso M, Piner RD, Adamson DH, et al. Functionalized graphene sheets for polymer nanocomposites. Nat Nanotechnol 2008;3:327–31.
[11] Steurer P, Wissert R, Thomann R, Mulhaupt R. Functionalized graphenes and thermoplastic nanocomposites based upon expanded graphite oxide. Macromol Rapid Commun 2009;30:316–27.
[12] Rafiee MA, Rafiee J, Wang Z, Song H, Yu ZZ, Koratkar N. Enhanced mechanical properties of nanocomposites at low graphene content. ACS Nano 2009;3:3884–90.
[13] Khan U, May P, O'Neill A, Coleman JN. Development of stiff, strong, yet tough composites by the addition of solvent exfoliated graphene to polyurethane. Carbon 2010;48:4035–41.
[14] Kim H, Miura Y, Macosko CW. Graphene/polyurethane nanocomposites for improved gas barrier and electrical conductivity. Chem Mater 2010;22:3441–50.
[15] Cai D, Yusoh K, Song M. The mechanical properties and morphology of a graphite oxide nanoplatelet/polyurethane composite. Nanotechnology 2009;20:085712.
[16] Zhao X, Zhang Q, Chen D. Enhanced mechanical properties of graphene-based poly(vinyl alcohol) composites. Macromolecules 2010;43:2357–63.
[17] Flandin L, Hiltner A, Baer E. Interrelationships between electrical and mechanical properties of a carbon black-filled ethylene–octene elastomer. Polymer 2001;42:827–38.
[18] Flandin L, Chang A, Nazarenko S, Hiltner A, Baer E. Effect of strain on the properties of an ethylene–octane elastomer with conductive carbon fillers. J Appl Polym Sci 2000;76:894–905.
[19] Maiti M, Sadhu S, Bhowmick AK. Ethylene–octene copolymer (Engage)–clay nanocomposites: preparation and characterization. J Appl Polym Sci 2006;101:603–10.
[20] Palza H. Effect of comonomer content on the behavior of propylene copolymer/compatibilizer/clay nanocomposites. Macromol Mater Eng 2010;295:492–501.
[21] Theravalappil R, Svoboda P, Vilcakova J, Poongavalappil S, Slobodian P, Svobodova D. A comparative study on the electrical, thermal and mechanical properties of ethylene–octene copolymer based composites with carbon fillers. Mater Des 2014;60:458–67.
[22] Kuila T, Bose S, Hong CE, Uddin ME, Khanra P, Kim NH, et al. Preparation of functionalized graphene/linear low density polyethylene composites by a solution mixing method. Carbon 2011;49:1033–51.
[23] Kim H, Kobayashi S, Abdur-Rahim MA, Zhang MJ, Khusainova A, Hillmyer MA, et al. Graphene/polyethylene nanocomposites: effect of polyethylene functionalization and blending methods. Polymer 2011;52:1837–46.
[24] Luyt AS, Molefi JA, Krump H. Thermal, mechanical and electrical properties of copper powder filled low-density and linear low-density polyethylene composites. Polym Degrad Stab 2006;91:1629–36.
[25] Xia X, Xie C, Cai S, Wen F, Zhu C, Yang X. Effect of the loading and size of copper particles on the mechanical properties of novel Cu/LDPE composites for use in intrauterine devices. Mater Sci Eng A 2006;429:329–33.
[26] Palza H, Gutiérrez S, Delgado K, Salazar O, Fuenzalida V, Avila J, et al. Toward tailor-made biocide materials based on polypropylene/copper nanoparticles. Macromol Rapid Commun 2010;31:563–7.
[27] Bensason S, Minick J, Moet A, Chum S, Hiltner A, Baer E. Classification of homogeneous ethylene–octene copolymers based on comonomer content. J Polym Sci Part B 1996;34:1301–15.
[28] Eynde SV, Mathot V, Koch MHJ, Reynaers H. Thermal behaviour and morphology of homogeneous ethylene–propylene and ethylene–1-butene copolymers with high comonomer contents. Polymer 2000;41:3437–53.
[29] Hummers W, Offeman R. Preparation of graphitic oxide. J Am Chem Soc 1958;80:1339. 1339.
[30] Garzon C, Palza H. Electrical behavior of polypropylene composites melt mixed with carbon-based particles: effect of the kind of particle and annealing process. Comp Sci Technol 2014;99:117–23.
[31] Kong Y, Hay JN. The measurement of the crystallinity of polymers by DSC. Polymer 2002;43:3873–8.
[32] Palza H, Lopez-Majada JM, Quijada R, Pereña JM, Benavente R, Perez E, et al. Comonomer length influence on the structure and mechanical response of metallocenic polypropylenic materials. Macromol Chem Phys 2008;209:2259–67.
[33] Palza H, Lopez-Majada JM, Quijada R, Benavente R, Perez E, Cerrada ML. Metallocenic copolymers of isotactic polypropylene and 1-octadecene: crystalline structure and mechanical behavior. Macromol Chem Phys 2005;206:1221–30.
[34] Xiao KQ, Zhang LC, Zarudi I. Mechanical and rheological properties of carbon nanotube-reinforced polyethylene composite. Comp Sci Technol 2007;67:177–82.
[35] Kim IH, Jeong YG. Polylactide/exfoliated graphite nanocomposites with enhanced thermal stability, mechanical modulus, and electrical conductivity.

J Polym Sci Part B 2010;48:850–8.
[36] Palza H, Vera J, Wilhelm M, Zapata P. Spherulite growth rate in polypropylene/silica nanoparticle composites: effect of particle morphology and compatibilizer. Macromol Mat Eng 2010;296:744–51.
[37] Song P, Cao Z, Cai Y, Zhao L, Fang Z, Fu S. Fabrication of exfoliated graphene-based polypropylene nanocomposites with enhanced mechanical and thermal properties. Polymer 2011;52:4001–10.
[38] Ghasemi AR, Mohammadi MM, Mohandes M. The role of carbon nanofibers on thermo-mechanical properties of polymer matrix composites and their effect on reduction of residual stresses. Compos Part B 2015;77:519–27.
[39] Kwon HJ, Sunthornvarabhas J, Park JW, Lee JH, Kim HJ, Piyachomkwan K, et al. Tensile properties of kenaf fiber and corn husk flour reinforced poly(lactic acid) hybrid bio-composites: role of aspect ratio of natural fibers. Compos Part B 2014;56:232–7.
[40] Banerjee S, Sankar BV. Mechanical properties of hybrid composites using finite element method based micromechanics. Compos Part B 2014;58:318–27.
[41] Shi DL, Feng XQ, Huang YY, Hwang KC, Gao H. The effect of nanotube waviness and agglomeration on the elastic property of carbon nanotube-reinforced composites. J Eng Mater Technol 2004;126:251–7.
[42] Yang QS, He XQ, Liu X, Leng FF, Mai YW. The effective properties and local aggregation effect of CNT/SMP composites. Compos Part B 2012;43:33–8.
[43] Palza H, Delgado K, Pinochet I. Improving the metal ion release from nanoparticles embedded in a polypropylene matrix for antimicrobial applications. J Appl Polym Sci 2015. http://dx.doi.org/10.1002/APP.41232.
[44] Kasaliwal GR, Goldel A, Potschke HG. Influences of polymer matrix melt viscosity and molecular weight on MWCNT agglomerate dispersion. Polymer 2011;52:1027–36.
[45] Yamada H, Manas-Zloczower I, Feke DL. Influence of matrix infiltration on the dispersion kinetics of carbon black agglomerates. Powder Technol 1997;92:163–9.
[46] Palza H, Quijada R, Wilhelm M. Effect of short-chain branching on the melt behavior of polypropylene under small-amplitude oscillatory shear conditions. Macromol Chem Phys 2013;214:107–16.
[47] Micusık M, Omastova M, Krupa I, Prokes J, Pissis P, Logakis E, et al. A comparative study on the electrical and mechanical behaviour of multiwalled carbon nanotube composites prepared by diluting a masterbatch with various types of polypropylenes. J Appl Polym Sci 2009;113:2536–51.
[48] Tjong SC. Structural and mechanical properties of polymer nanocomposites. Mater Sci Eng R 2006;53:73. 197.
[49] Palza H, Vergara R, Zapata P. Composites of polypropylene melt blended with synthesized silica nanoparticles. Comp Scie Technol 2011;71:535–40.
[50] Sanders PG, Eastman JA, Weertman JR. Elastic and tensile behavior of nanocrystalline copper and palladium. Acta mater 1997;45:4019–25.
[51] Bedoui F, Diani J, Regnier G. Micromechanical modeling of elastic properties in polyolefins. Polymer 2004;45:2433–42.
[52] Thiruppukuzhi SV, Sun CT. Models for the strain-rate-dependent behavior of polymer composites. Compos Sci Technol 2001;61:1–12.
[53] Odegard GM, Pipes RB, Hubert P. Comparison of two models of SWCN polymer composites. Compos Sci Technol 2004;64:1011–20.
[54] Shaat M, Abdelkefi A. Size dependent and micromechanical modeling of strain gradient-based nanoparticle composite plates with surface elasticity. Eur J Mech - A/Solids 2016;58:54–68.